($CN^- \rightarrow CNO^-$), or a catalyst ($Ru^{III}/CN^- \rightarrow Ru^{II}/CNO^-$), experiments were performed to measure the yield of O_2. It was found that 0.5 mol of O_2 was produced/mol of H_2O_2 used, the result expected if H_2O_2 produces O_2 only via disproportionation to H_2O and O_2. It is therefore proposed that a reaction sequence similar to the following occurs in alkaline solutions containing $Ru(CN)_6^{3-}$ and H_2O_2.

$$Ru(CN)_6^{3-} + H_2O_2 \rightarrow Ru(CN)_6^{4-} + HO_2 + H^+$$

$$Ru(CN)_6^{3-} + HO_2 \rightarrow (NC)_5Ru(CNOOH)^{3-}$$

$$(NC)_5Ru(CNOOH)^{3-} + H_2O \rightarrow (NC)_5Ru(CNO)^{4-} + H_2O_2 + H^+$$

net: $2Ru(CN)_6^{3-} + H_2O \rightarrow Ru(CN)_6^{4-} + (NC)_5Ru(CNO)^{4-} + 2H^+$

The hydrogen peroxide is simultaneously decomposed by disproportionation via catalysis by an appropriate Ru^{II}/Ru^{III} couple.

Stoichiometry of $Ru(CN)_6^{3-} + OH^-$. Failure to detect either H_2O_2 or O_2 as reaction products in alkaline solutions of $Ru(CN)_6^{3-}$ (vide supra) suggests that oxygen is being incorporated into the system via oxidation of a cyano ligand. The reaction sequence (15) and (16) is postulated where L = $(NCOH)^{2-}$ or $(CNOH)^{2-}$ depending on the position of attack of OH^-. The net reaction thus corresponds to the oxidation by Ru(III) of ligand cyanide to ligand cyanate (or an isomer thereof).

$$Ru^{III}(CN)_6^{3-} + OH^- \rightarrow (NC)_5Ru^{III}(L)^{4-} \quad (15)$$

$$OH^- + Ru^{III}(CN)_6^{3-} + (NC)_5Ru^{III}(L)^{4-} \rightarrow Ru^{II}(CN)_6^{4-} + Ru^{II}(CN)_5(NCO)^{4-} + H_2O \quad (16)$$

Support for the overall stoichiometry shown in eq 15 and 16 has been obtained by acid hydrolysis of the solutions resulting from the treatment of $Ru(CN)_6^{3-}$ with OH^-; NH_4^+ and CO_2 are produced as would be expected from the known reaction $NCO^- + 2H^+ + H_2O \rightarrow CO_2 + NH_4^+$. In eight such experiments, recovery of CO_2 ranged from 95 to 101% of the expected amount and of NH_4^+ from 78 to 102% (with five of the eight values in the range 98-102%). These results require that OH^- attack the carbon atom of the cyano ligand (or that attack at nitrogen is followed by isomerization to an N-C-O moiety). Spectral observations (with and without reoxidation by Ce(IV)) also require that the postulated (isocyanato)pentacyanoruthenium(II) and -ruthenium(III) species have UV/vis spectra similar to those of the corresponding hexacyanides.

Acknowledgment. The contribution of Mark Westerhoff to the cyanate hydrolysis and Ce(IV) reoxidation studies is gratefully acknowledged. The work was supported by the Illinois Institute of Technology and Saint Xavier College.

Registry No. $(NH_4)_4Ce(SO_4)_4$, 7637-03-8; $Ru(CN)_6^{4-}$, 21029-33-4; $Ru(CN)_6^{3-}$, 54692-27-2; CN^-, 57-12-5; $HgCl_2$, 7487-94-7; $Ru^{III}(CN)_5(OH_2)^{2-}$, 74009-26-0; MnO_4^-, 14333-13-2; PbO_2, 1309-60-0; H_2O_2, 7722-84-1; OH^-, 14280-30-9.

Contribution from the Department of Chemistry, City University of New York, Queens College, Flushing, New York 11367

Spectroscopic and Electrochemical Properties of the Dimer Tetrakis(2,2'-bipyridine)(μ-2,3-bis(2-pyridyl)pyrazine)diruthenium(II) and Its Monomeric Analogue

CARLOS H. BRAUNSTEIN, A. DAVID BAKER,* THOMAS C. STREKAS,* and HARRY D. GAFNEY*

Received June 7, 1983

The ligand 2,3-bis(2-pyridyl)pyrazine, dpp, has been used to prepare the complexes $Ru(bpy)_2(dpp)^{2+}$ and $(bpy)_2Ru(dpp)Ru(bpy)_2^{4+}$. In contrast to previously synthesized mono- and bimetallic Ru(II) complexes, both $Ru(bpy)_2(dpp)^{2+}$ and $(bpy)_2Ru(dpp)Ru(bpy)_2^{4+}$ are luminescent in room-temperature fluid solution. The resonance Raman spectra of the complexes exhibit a pronounced dependence on excitation wavelength, which indicates that the visible MLCT transitions terminate in different ligands. Luminescence is assigned to a dpp π^*-Ru(II) t_2 transition, and measurements of the relative quantum yields of emission indicate that the emissive state is populated with equal efficiency in both complexes. Analysis of the electrochemical and spectral properties of the complexes indicates that the perturbation introduced by the second $Ru(bpy)_2^{2+}$ moiety in $(bpy)_2Ru(dpp)Ru(bpy)_2^{4+}$ is relatively small and similar to that introduced by substituting a weak electron-withdrawing substituent onto the ligand periphery. This relatively weak interaction, which is thought to be the reason both mono- and bimetallic complexes emit, is attributed to steric constraints imposed by the dpp bridging ligand.

Introduction

Recognition of the photoinduced redox properties of tris(2,2'-bipyridine)ruthenium(II), $Ru(bpy)_3^{2+}$,[1] has spurred numerous studies of the complex and related derivatives, which have led to a rather detailed understanding of this chemistry.[2-5] Optical excitation of the complex leads to population of a luminescent metal to ligand charge-transfer (MLCT) state, which can act as an oxidizing or reducing agent.[2,3,5] Current interest centers on minimizing the reverse reaction that follows the photoinduced electron transfer and converting the one-photon, one-electron redox steps into more useful multielectron-transfer reactions. Semiconductors, electron relay reagents, and catalysts are being investigated as a means of storing electrons and initiating subsequent multielectron reactions.[4] Another approach is the use of dimeric Ru(II) complexes, which, if certain lifetime constraints are satisfied, could in principle act as a two-electron-transfer reagent when excited by two photons. Although a number of dimeric Ru(II) complexes have previously been prepared for the purpose of studying the intervalence charge-transfer (IT) transition in the mixed-valence (+5) system,[6-13] none satisfy the criteria

(1) Gafney, H. D.; Adamson, A. W. *J. Am. Chem. Soc.* **1972**, *94*, 8238.
(2) Bock, C. R.; Meyer, T. J.; Whitten, D. G. *J. Am. Chem. Soc.* **1974**, *96*, 4710.
(3) Navon, G.; Sutin, N. *Inorg. Chem.* **1974**, *13*, 2159.
(4) Kalyanasundaram, K. *Coord. Chem. Rev.* **1982**, *46*, 159.
(5) Creutz, C.; Sutin, N. *Inorg. Chem.* **1976**, *15*, 496.
(6) Creutz, C.; Taube, H. *J. Am. Chem. Soc.* **1969**, *91*, 3988.
(7) Creutz, C.; Taube, H. *J. Am. Chem. Soc.* **1972**, *95*, 1086.
(8) Elias, J. H.; Drago, R. S. *Inorg. Chem.* **1972**, *11*, 415.
(9) Callahan, R. W.; Brown, G. M.; Meyer, T. J. *J. Am. Chem. Soc.* **1974**, *96*, 7829.
(10) Callahan, R. W.; Brown, G. M.; Meyer, T. J. *Inorg. Chem.* **1975**, *14*, 1443.
(11) Tom, G. M.; Taube, H. *J. Am. Chem. Soc.* **1975**, *97*, 5310.

0020-1669/84/1323-0857$01.50/0

of field strength and/or coordination about each Ru(II) ion necessary for luminescence. Luminescence is not necessarily a prerequisite for photoredox behavior, but its presence is a desired property as a convenient probe of the excited state and its redox potentials.

Studies with previously synthesized Ru(II) dimers suggest that, in general, deviations from a bipyridine-like structure in the bridging ligand cause a loss of the d–π^* luminescence characteristic of $Ru(bpy)_3^{2+}$ and its homologues. For example, Dose and Wilson,[14] Hunziker and Ludi,[15] and Rillema and Meyer[16] report that although the monomer $Ru(bpy)_2(bpm)^{2+}$ (bpm denotes 2,2′-bipyrimidine) is luminescent when dissolved in room-temperature acetonitrile solution, the corresponding bridged dimer $(bpy)_2Ru(bpm)Ru(bpy)_2^{4+}$ is not. Rillema and Meyer[16] also report similar results for $(bpy)_2RuLRu(bpy)_2^{4+}$, where L is 2,2′-bibenzimidazole or 2,3-bis(2-pyridyl)-quinoxaline. Weak emissions are observed from ambient-temperature fluid solutions of the monometallic $(bpy)_2RuL^{2+}$ complexes whereas the bimetallic complexes do not emit under similar conditions.

Our interest has centered on the preparation of bimetallic Ru(II) complexes which are likely to be luminescent in ambient-temperatue fluid solution. The above data suggest that what appear to be, a priori, slight differences in structure are sufficient to prevent luminescence. Consequently, preparation of luminescent bimetallic Ru(II) complexes demands a bridging ligand that resembles, as closely as possible, 2,2′-bipyridine so that the coordination and field strength about each Ru(II) ion is essentially equivalent to that in $Ru(bpy)_3^{2+}$. For this reason we have synthesized 2,3-bis(2-pyridyl)pyrazine, designated dpp, and in this paper, we describe the preparation and the spectral and electrochemical properties of its monometallic, $Ru(bpy)_2(dpp)^{2+}$, and bimetallic, $(bpy)_2Ru(dpp)Ru(bpy)_2^{4+}$, complexes.

In contrast to previously synthesized complexes,[14-17] both the mono- and bimetallic complexes of dpp are luminescent in room-temperature fluid solution. Resonance Raman spectra of $Ru(bpy)_2(dpp)^{2+}$ and $(bpy)_2Ru(dpp)Ru(bpy)_2^{4+}$ establish that the visible absorptions of the complexes are MLCT transitions that lead to population of the π^* orbitals in the different ligands. The relative luminescence quantum yields indicate an efficient interconversion amongst these π^* orbitals, and the luminescence of both mono- and bimetallic complexes is assigned to a π^*–t_2 transition in which the lowest energy π^* orbital is principally localized on the dpp ligand. The spectral and electrochemical data gathered in these experiments indicate minimal metal–metal interaction in $(bpy)_2Ru(dpp)Ru(bpy)_2^{4+}$ in both ground and excited states. This contrasts with previously synthesized bimetallic complexes,[14-17] where there is significant interaction, and is thought to be the cause of the difference in their emission properties. The minimal interaction in $(bpy)_2Ru(dpp)Ru(bpy)_2^{4+}$ is attributed to steric constraints imposed by dpp, which prevent the coordination octahedra about each Ru(II) ion from being coplanar.

Experimental Section

Materials. $[Ru(bpy)_3]Cl_2 \cdot 3H_2O$ was prepared according to the procedure of Palmer and Piper,[18] and the absorption and emission spectra of the recrystallized sample are in excellent agreement with published spectra.[19,20] $[Os(bpy)_3]Cl_2 \cdot 3H_2O$ was prepared and purified according to previously described procedures[21,22] and converted to the perchlorate salt by recrystallization from aqueous $NaClO_4$ solutions. The absorption and emission spectra of twice-recrystallized $[Os(bpy)_3](ClO_4)_2$ were in excellent agreement with published spectra.[20]

2,3-Bis(2-pyridyl)pyrazine was prepared according to the procedure of Goodwin and Lions.[23] A 56-mmol amount of ethylenediamine (Aldrich) and 59 mmol of 2,2′-pyridil (Aldrich) were refluxed in 15 mL of ethanol for 3 h. After the reaction mixture was cooled, light yellow crystals of 2,3-bis(2-pyridyl)-5,6-dihydropyrazine were filtered off and recrystallized from ethanol. A 42-mmol amount of the crystalline 2,3-bis(2-pyridyl)-5,6-dihydropyrazine (mp 185–187 °C, lit.[23] mp 188 °C) was dissolved in 125 mL of mesitylene and refluxed for 20 h with a slurry of 10% Pd on charcoal (Colonial Metals Inc.). The hot reaction mixture was then filtered, and the crude product was precipitated by cooling the filtrate. After filtration and recrystallization from ethanol, 2,3-bis(2-pyridyl)pyrazine was obtained in 54% yield: mp 163–165 °C, lit.[23] mp 167 °C.

The monometallic complex was prepared by refluxing equimolar amounts of *cis*-$Ru(bpy)_2Cl_2$[24] and dpp in 95% ethanol for 72 h. The dark red reaction mixture was filtered while hot, and the product was precipitated from the cooled filtrate by addition of an aqueous solution of $NaClO_4$. The complex was purified by repeated recrystallizations from a 1:1 water–ethanol solution. Anal. Calcd for $[Ru(bpy)_2(dpp)](ClO_4)_2 \cdot 2H_2O$: C, 46.27; H, 3.43; N, 12.69. Found: C, 46.11; H, 3.49; N, 11.98.

The bimetallic complex was prepared in a similar manner except that 2 equiv of *cis*-$Ru(bpy)_2Cl_2$ was refluxed with 1 equiv of dpp in 95% ethanol for 72 h. After the reaction mixture was filtered and cooled, a reddish purple solid was precipitated by addition of $NaClO_4$ solution. An absorption spectrum of this material after recrystallization from 1:1 water–ethanol showed a 450-nm band, indicating the presence of the monometallic as well as bimetallic complex. Although repeated recrystallization of the bimetallic complex did reduce the 450-nm absorption to a negligible amount, $A_{450} \leq 0.003$, emission spectra of the recrystallized samples continued to indicate the presence of traces of the mononuclear complex. These spectra, which consisted of emission bands centered at 650 nm, equivalent to that found for the mononuclear complex, and 750 nm, indicated that as many as 10 recrystallizations of the dinuclear complex reduced the amount of the monometallic analogue to some minimum amount but failed to completely eliminate it. To obtain pure samples, the recrystallized mono- and bimetallic complexes were further purified by chromatography.[25]

Concentrated acetonitrile solutions of the monometallic and the bimetallic complexes were charged onto 100 cm × 2 cm diameter silica gel columns and eluted with 0.5 M ethanol solutions of $(C_2H_5)_4NBr$. Elution of the monometallic complex showed that a small amount of darkly colored material remained at the top of the column while the majority was eluted as a single dark red band, which was isolated and evaporated to dryness. The residue was dissolved in a minimum of warm ethanol, and the mononuclear complex precipitated on cooling. The absorption spectrum of this sample purified by the chromatographic procedure was in excellent agreement with the spectrum of the product purified by recrystallization.

Elution of the bimetallic complex, however, showed that, in addition to the material that remained at the top of the column, two bands were developed on the column. The first band eluted from the column was dark red, and absorption spectra of the eluted fraction established that it contained the monometallic complex. The second band was purple, and absorption spectra of this eluate showed no absorption at 450 nm. Furthermore, emission spectra of this fraction gave a single emission band centered at 750 nm. This fraction was evaporated to dryness and taken up in a minimum of warm ethanol and the bimetallic complex precipitated by addition of $NaClO_4$. The samples of the bimetallic complex used in these studies were purified by this chro-

(12) Krentzien, H.; Taube, H. *J. Am. Chem. Soc.* **1976**, *98*, 6379.
(13) Powers, M. J.; Callahan, R. W.; Salmon, D. J.; Mayer, T. J. *Inorg. Chem.* **1976**, *15*, 894.
(14) Dose, E. V.; Wilson, K. J. *Inorg. Chem.* **1978**, *17*, 2660.
(15) Hunziker, M.; Ludi, A. *J. Am. Chem. Soc.* **1977**, *99*, 7370.
(16) Rillema, D. P.; Meyer, J. "Abstracts of Papers", 179th National Meeting of the American Chemical Society, Houston, TX, March 1980; American Chemical Society: Washington, DC, 1980; INOR 30.
(17) Tinnemans, A. H. A.; Timmer, K.; Reintein, M.; Kraaijkamp, J. G.; Alberts, A. H. van der Linden, J. G. M.; Schmitz, J. E. J.; Saaman, A. A. *Inorg. Chem.* **1981**, *20*, 3698.
(18) Palmer, R. A.; Piper, T. S. *Inorg. Chem.* **1966**, *5*, 864.
(19) Fujita, I.; Kobayashi, H. *Inorg. Chem.* **1973**, *12*, 2758.
(20) Fabian, R. H.; Klassen, D. M.; Sonntag, R. W. *Inorg. Chem.* **1980**, *19*, 1977.
(21) Burstall, F. H.; Dwyer, F. P.; Gyarafs, E. C. *J. Chem. Soc.* **1950**, 953.
(22) Liu, C. F.; Liu, N. C.; Bailar, J. C. *Inorg. Chem.* **1964**, *3*, 1085.
(23) Goodwin, H. A.; Lions, F. *J. Am. Chem. Soc.* **1959**, *81*, 6415.
(24) Sullivan, B. P.; Salmon, D. J.; Mayer, T. *Inorg. Chem.* **1978**, *17*, 3334.
(25) We thank Drs. R. A. Krause and K. Krause of the University of Connecticut (Storrs, CT) for developing and sharing with us this technique.

matographic procedure. Anal. Calcd for $[(bpy)_2Ru(dpp)Ru(bpy)_2](ClO_4)_4 \cdot 5H_2O$: C, 41.87; H, 3.38; N, 10.85. Found: C, 41.79; H, 3.14; N, 10.51.

Physical Measurements. Absorption spectra were recorded on a Cary 14 spectrophotometer or a Perkin-Elmer Lambda 3 UV/vis spectrophotometer. Emission spectra were recorded on a Perkin-Elmer Hitachi MPF-2A emission spectrophotometer equipped with a red-sensitive Hamamatsu R818 photomultiplier. For ambient-temperature emission spectra, solutions contained in 1 cm × 1 cm quartz cells were deaerated by N_2 or He bubbling or degassed by repetitive freeze–pump–thaw cycles. For low-temperature (77 K) emission spectra, the solutions were placed in 2 mm diameter quartz tubes and mounted in a quartz Dewar filled with liquid N_2.

To determine the intersystem crossing efficiencies, relative emission quantum yields, ϕ_{em}, for $Ru(bpy)_2(dpp)^{2+}$ and $(bpy)_2Ru(dpp)Ru(bpy)_2^{4+}$ were measured as a function of excitation wavelengths according to the procedure described by Demas and Crosby.[26] In these measurements, $[Os(bpy)_3](ClO_4)_2$,[20] rather than other Ru(II) polypyridine complexes, was used as a standard since the broad absorption spectrum and low-energy emission spectrum of the Os(II) complex overlap the respective spectra of the Ru(II) mono- and bimetallic complexes. The concentrations of methanol solutions of the monomer and dimer were adjusted to have an absorbance through a 1-cm cell of ≤0.4 at the excitation wavelength. The concentrations of ethanol solutions of $[Os(bpy)_3](ClO_4)_2$ were also adjusted so that at each excitation wavelength the absorbance was ≤0.4 and differed from that of the Ru(II) solution by ≤15%. After deaeration by N_2 bubbling, the emission intensity from the Ru(II) solution, I_{em}^r, was measured at the emission maximum of the complex and then the emission intensity from the deaerated ethanol solution of $[Os(bpy)_3](ClO_4)_2$ was measured under identical conditions. The process was repeated for the different excitation wavelengths, and three measurements of I_{em}^r and I_{em}^o were made at each excitation wavelength. The values of ϕ_{em} were calculated from the emitted intensity according to the equation

$$\phi_{em} = \phi_0(1 - 10^{-A(r)})I_{em}^r/(1 - 10^{-A(o)})I_{em}^o \quad (1)$$

where $A(r)$ and $A(o)$ are the absorbances of the Ru(II) and Os(II) solutions, respectively, at each excitation wavelength. The value of ϕ_0 was assumed to be equal to the quantum yield of emission from $[Os(bpy)_3]I_2$, 0.0348 ± 0.0020.[26] In addition to different counterions—the perchlorate salt was used in these experiments—the latter value was measured in a methanol glass at 77 K[26] whereas the emission intensities measured in these experiments were from deaerated, room-temperature (22 ± 1 °C) ethanol solutions of the complexes. Consequently, the calculated values of ϕ_{em}, which are most likely high estimates of the actual quantum yields, can only be used in a relative sense to indicate the intersystem crossing efficiencies from the different excited states populated on absorptions.

The resonance Raman spectrophotometer has been previously described.[27] Spectra of H_2O or CH_3CN solutions of the complexes in glass capillary tubes or 3-mm square, flat-bottomed cells were obtained by means of 90° transverse excitation. Optical spectra recorded before and after the Raman spectra established that the laser excitation used to record the Raman spectra did not cause an irreversible chemical change.

Cyclic voltammetry measurements were made with a PAR electrochemistry system that consists of a Model 364 polarographic analyzer driven by a Model 175 universal programmer. All measurements were made at a sweep rate of 200 mV/s, and the analyzer output was displayed on a Houston Instruments Omnigraphic Model 2000 XY recorder. Millimolar solutions of the Ru(II) complexes (as ClO_4^- salts) were prepared in 0.1 M acetonitrile solutions of tetraethylammonium perchlorate. The acetonitrile was freshly distilled over P_2O_5, and the solutions were deaerated by bubbling with dry N_2. All measurements were made under an N_2 atmosphere with a Pt-microcylinder working electrode, a Pt-wire auxiliary electrode, and a standard Ag/AgCl reference electrode.

Luminescent decay measurements were made by N_2 laser excitation of room-temperature (22 ± 1 °C), aqueous solutions of the Ru(II) complexes. A 1-cm cell that contained (2–5) × 10^{-5} M solutions of the Ru(II) complexes was deaerated by N_2 bubbling and excited at 337.1 nm by a Lumonics N_2 laser (fwhm = 12 ns). The emission decay was monitored at right angles to the excitation through a 0.25-m Jarrel-Ash grating monochromator with an RCA C31034A-02 photomultiplier. The photomultiplier tube was mounted in a Products For Research thermoelectrically cooled housing and powered by a Bertan Associates Model 215 power supply. The photomultiplier current was displayed as a function of time either directly on a Tektronix Model 7834 scope with a 50-Ω input impedence Model 7A29 vertical amplifier or indirectly into a PAR Model 162 boxcar averager equipped with a Model 164 gated integrator, with the output of the averager then being displayed on the above scope. The sweep of the scope or the boxcar averager was triggered off the laser discharge, and the trace was photographed with a Tektronix Model C-51 oscilloscope camera. The emission intensity was measured from the photographs and plotted according to first-order kinetics.

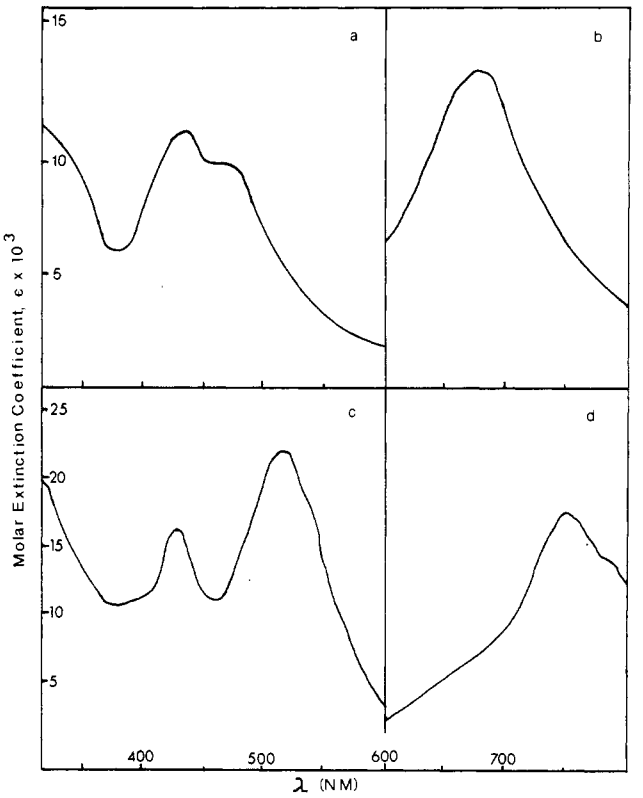

Figure 1. Absorption (a) and emission (b) spectra for a room-temperature fluid solution of $(bpy)_2Ru(dpp)^{2+}$ and absorption (c) and emission (d) spectra for a room-temperature fluid solution of $(bpy)_2Ru(dpp)Ru(bpy)_2^{4+}$.

Results

Absorption and Emission Spectra. $Ru(bpy)_2(dpp)^{2+}$ and $(bpy)_2Ru(dpp)Ru(bpy)_2^{4+}$ have similar UV spectra, which, like those of other Ru(II) polypyridine complexes,[28,29] consist of a series of intense ($\epsilon \approx 10^4$–10^5 M^{-1} cm^{-1}) absorptions within the ligand π–π^* system. The visible absorption spectra of the mono- and bimetallic complexes are dominated by the intense absorptions characteristic of all Ru(II) polypyridine complexes. The spectrum of $Ru(bpy)_2(dpp)^{2+}$ shown in Figure 1a consists of an intense ($\epsilon = 1.2 \times 10^4$ M^{-1} cm^{-1}) absorption with a maximum at 430 nm and a shoulder, although not well resolved, at ca. 470 nm. In contrast, the visible absorption spectrum of $(bpy)_2Ru(dpp)Ru(bpy)_2^{4+}$ shown in Figure 1c consists of two well-resolved absorption bands with maxima at 425 nm ($\epsilon = 1.7 \times 10^4$ M^{-1} cm^{-1}) and 525 nm ($\epsilon = 2.1 \times 10^4$ M^{-1} cm^{-1}).

The emission spectrum of ambient-temperature, deaerated, fluid solutions of the monometallic complex, as shown in Figure

(26) Demas, J. N.; Crosby, G. A. *J. Am. Chem. Soc.* **1971**, *93*, 2841.
(27) Knorrs, C.; Gafney, H. D.; Baker, A. D.; Braunstein, C. H.; Strekas, T. C. *J. Raman Spectrosc.* **1983**, *14*, 32.
(28) Crosby, G. A. *Acc. Chem. Res.* **1975**, *8*, 231.
(29) Balzani, V.; Boletta, E.; Gandolfi, M. T.; Maestri, M. *Top. Curr. Chem.* **1978**, *75*, 1.

Table I. Relative Quantum Yields of Emission[a]

	λ_{ex}, nm	ϕ_{em}[b]
$(bpy)_2Ru(dpp)^{2+}$	436	0.049 ± 0.006
	465	0.051 ± 0.005
	475	0.045 ± 0.005
$(bpy)_2Ru(dpp)Ru(bpy)_2^{4+}$	425	0.0029 ± 0.0003
	436	0.0031 ± 0.0003
	525	0.0027 ± 0.0004

[a] All data are for ethanol solutions of the complexes deaerated by N_2 bubbling. [b] Emission from $(bpy)_2Ru(dpp)^{2+}$ monitored at 675 nm and that from $(bpy)_2Ru(dpp)Ru(bpy)_2^{4+}$ at 755 nm.

1b, consists of a single emission band with a maximum at 675 nm. The excitation spectrum of the emission closely resembles the visible absorption spectrum and indicates that excitation of either the 430-nm maximum or the 470-nm shoulder leads to population of the emissive state. The emission intensity is slightly dependent on O_2 concentration and decreases ~10% when the solution is saturated with air. Freezing the solutions in liquid N_2 (77 K) decreases the half-width of the emission band slightly but does not resolve a superimposed vibrational progression.

The emission properties of the bimetallic complex resemble those of the monometallic analogue, although the emitted intensity, corrected for the spectral response of the photomultiplier, is ~10% of that of the monometallic complex. As shown in Figure 1d, the emission spectrum of the bimetallic complex consists of a single band with a maximum at 755 nm. The excitation spectrum of the emission closely resembles the absorption spectrum of the complex and indicates that excitation of either the 425- or the 520-nm visible absorption leads to population of the emissive state. Saturating the solution with air does not change the emission intensity beyond experimental error. Freezing the solution in liquid N_2 slightly decreases the half-width of the emission band but does not resolve a vibrational progression.

The emission quantum yields for $Ru(bpy)_2(dpp)^{2+}$ and $(bpy)_2Ru(dpp)Ru(bpy)_2^{4+}$ in ethanol solutions deaerated by N_2 bubbling, listed in Table I, are calculated relative to the emission quantum yield of $[Os(bpy)_3]I_2$ and as such are most likely high estimates of the actual quantum yields for emission from room-temperature ethanol solution. In a relative sense, however, the values of ϕ_{em} for both the mono- and bimetallic complexes are independent of the excitation wavelength. In view of the results of detailed studies on other Ru(II) polypyridine complexes by Demas and Crosby,[26] the absence of a dependence of ϕ_{em} on the excitation wavelength suggests that the intersystem crossing efficiencies, ϕ_{isc}, from the initially populated states are equivalent. These data do not specify that ϕ_{isc} is unity but rather that in the bimetallic complex in particular where the visible absorptions are well resolved and, as described below, excitation leads to population of π^* orbitals in different ligands, crossing from these different ligand states appears to occur with the same efficiency. Comparing the valus of ϕ_{em} calculated for the dimer with those of the monomer indicates that the second $Ru(bpy)_2$ moiety, while not affecting the intersystem crossing efficiencies, does exert a substantial effect on the radiative and/or nonradiative decay of the luminescent state.

The emissions of the mononuclear and dinuclear complexes decay via first-order processes when ambient-temperature, aqueous solutions are excited at 337.1 nm with an N_2 laser. The laser wavelength corresponds to the onset of the ligand $\pi-\pi^*$ transitions, but excitation of these transitions in both complexes leads to the above emissions. Figure 2 is representative of first-order plots of emitted intensity, monitored at the respective emission maxima, vs. time for aqueous solutions deaerated by N_2 bubbling. For $Ru(bpy)_2(dpp)^{2+}$ (Figure 2a) the slopes of these plots yield an average emission

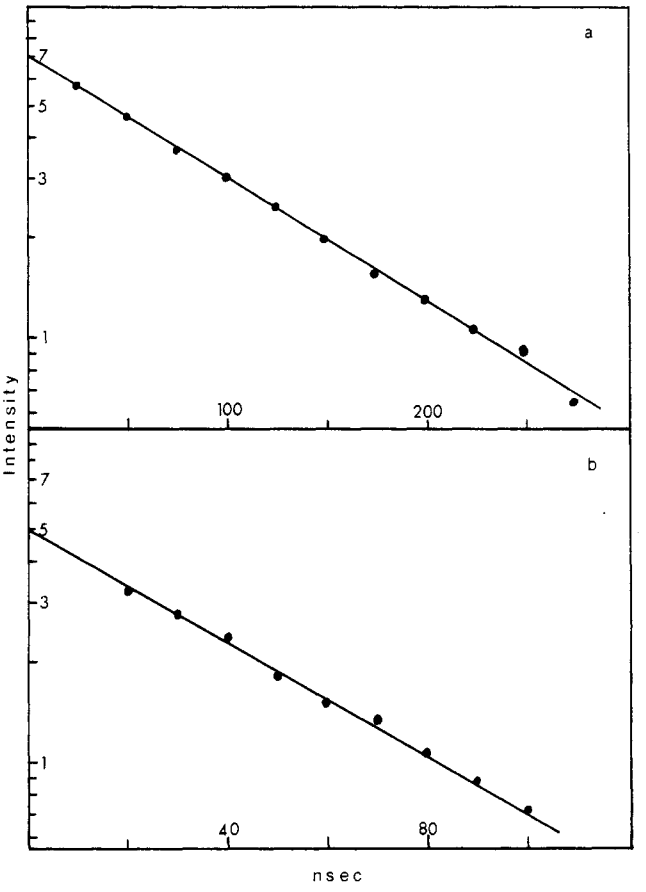

Figure 2. First-order plots of the luminescence decays following 337.1-nm excitation of N_2-flushed aqueous solutions: (a) 3.0×10^{-5} M $[(bpy)_2Ru(dpp)](ClO_4)_2$ monitored at 688 nm; (b) 4.93×10^{-5} M $[(bpy)_2Ru(dpp)Ru(bpy)_2](ClO_4)_4$ monitored at 770 nm.

decay rate constant, k_{em}, of $(7.41 \pm 0.70) \times 10^6$ s^{-1} and a corresponding lifetime of 135 ± 14 ns. Similarly, plots of the decay of $(bpy)_2Ru(dpp)Ru(bpy)_2^{4+}$ emission (Figure 2b) yield $k_{em} = (1.89 \pm 0.36) \times 10^7$ s^{-1} and a lifetime of 54 ± 11 ns. Saturating the solutions with air, ca. 2×10^{-4} M in O_2, decreases the lifetime of the monometallic complex to 105 ± 10 ns but, consistent with the more rapid emission decay rate, has no effect beyond experimental error on the lifetime of the bimetallic complex.

Comparing photographs of the laser pulse with the rise of the $Ru(bpy)_2(dpp)^{2+}$ emission indicates an emission rise time of ≤5 ns. However, a similar estimate of the emission rise time of the bimetallic complex is difficult. Because of the lower emission intensity from the bimetallic complex, the photomultiplier current is fed into a PAR boxcar averager and then displayed on the scope. This improves the signal to noise ratio to ca. 10:1 but superimposes on the initial portion of the signal the rise time of the boxcar averager. Consequently, these data indicate an emission rise time of ≤10 ns. However, we believe that the emission rise times of both the mono- and bimetallic complexes are ≤1 ns. This is based on measurements of the rise and decay of the emission from $Ru(bpy)_3^{2+}$ in deaerated, aqueous solutions undertaken to establish the reliability of measurements with the boxcar averager. Previous experiments with deaerated, aqueous solutions of $Ru(bpy)_3^{2+}$ indicate a rise time of ≤0.1 ns and an emission lifetime of 600 ± 20 ns.[20,26,30] Similar measurements during the course of these experiments yield a $Ru(bpy)_3^{2+}$ emission lifetime of 617 ± 20 ns. Furthermore, since the rise of the $Ru(bpy)_2(dpp)^{2+}$ and $(bpy)_2Ru(dpp)Ru(bpy)_2^{4+}$ emissions coincides with the rise

(30) Elfring, W. H.; Crosby, G. A. *J. Am. Chem. Soc.* **1981**, *103*, 2683.

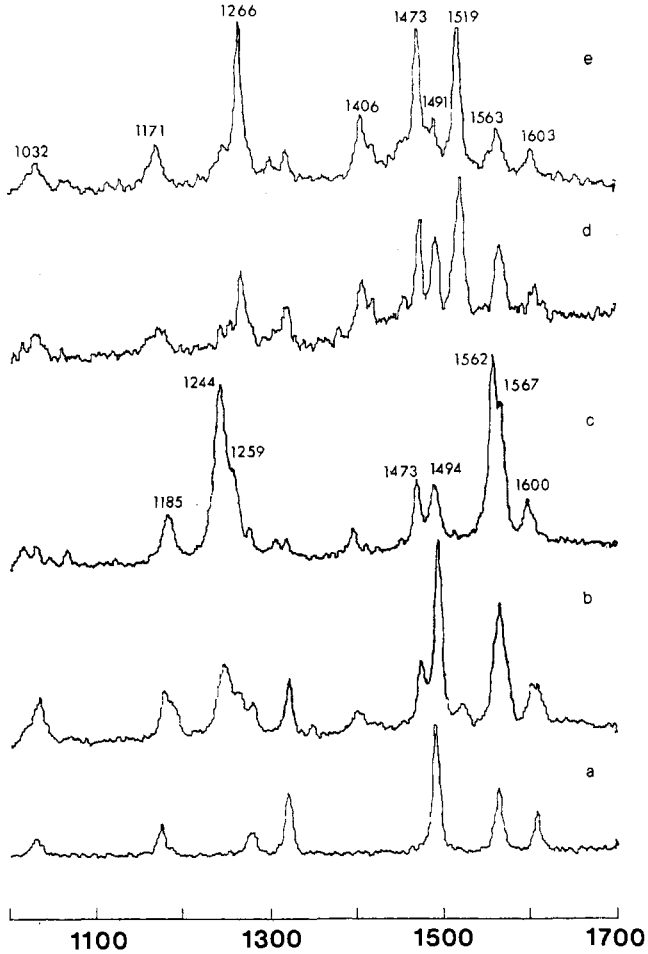

Figure 3. Resonance Raman spectra for (a) $Ru(bpy)_3^{2+}$ excited at 457.9 nm, (b) $(bpy)_2Ru(dpp)Ru(bpy)_2^{4+}$ excited at 457.9 nm, (c) $(bpy)_2Ru(dpp)Ru(bpy)_2^{4+}$ excited at 514.5 nm, (d) $(bpy)_2Ru(dpp)^{2+}$ excited at 457.9 nm, and (e) $(bpy)_2Ru(dpp)^{2+}$ excited at 488.0 nm. In all cases, a laser power of 40 mW and a spectral slit width of 4 cm^{-1} were used.

of the $Ru(bpy)_3^{2+}$ emission, a conservative estimate of the emission rise times of both complexes is ≤ 1 ns.

Resonance Raman Spectra. Previous studies show that laser excitation in the intense visible absorption bands of bis- and tris(polypyridine)ruthenium(II) complexes yield detailed resonance Raman spectra that above 1000 cm^{-1}, consist of a series of vibrations characteristic of aromatic diimine ligands.[27,31,32] The spectrum of $Ru(bpy)_3^{2+}$ shown in Figure 3a consists of seven bipyridine vibrations in the 1000–1700-cm^{-1} region, and aside from the slight changes in the relative intensities, excitation of the complex with different Ar laser lines that overlap the MLCT absorption to varying degrees yield spectra in which the bipyridine vibrations differ by ≤ 2 cm^{-1}. Resonance Raman spectra of the bis(bipyridine) complexes, $Ru(bpy)_2X_2$, where X is a monodentate ligand such as chloride, are also independent of the excitation wavelength even though the visible absorption spectrum consists of two relatively intense ($\epsilon \approx 10^3$ M^{-1} cm^{-1}) absorptions. Excitation of these complexes with different Ar and Kr laser lines, which span both absorption bands, yield the seven-vibration pattern characteristic of the bipyridine ligand.[33]

In contrast to the above results, in which the spectra are independent of excitation wavelength, the resonance Raman spectra of $Ru(bpy)_2(dpp)^{2+}$ and $(bpy)_2Ru(dpp)Ru(bpy)_2^{4+}$ exhibit a revealing dependence on the excitation wavelength. The visible absorption spectrum of the mononuclear complex, as noted above, consists of an intense absorption at 430 nm with a distinct shoulder at 470 nm. Excitation of the complex with the 457.9-nm Ar laser line, which is intermediate between the absorption maximum and the shoulder, yields the resonance Raman spectrum shown in Figure 3d. Comparing this spectrum with that of $Ru(bpy)_3^{2+}$ shows that the seven bipyridine vibrations are present along with additional vibrations most notably at 1266, 1473, and 1519 cm^{-1}. Since these last vibrations lie within the region expected for aromatic diimine ligands and are not present in the $Ru(bpy)_3^{2+}$ spectrum, they are assigned to the dpp ligand. As the excitation wavelength traverses the visible absorptions of $Ru(bpy)_2(dpp)^{2+}$, the spectrum in Figure 3e (488.0-nm excitation) shows that the intensities of the dpp vibrations increase relative to the intensities of the bpy vibrations. For example, the ratio of intensities of the 1519-cm^{-1} dpp vibration relative to the 1491-cm^{-1} bpy vibration increases from ~ 2 to ~ 8 when the excitation wavelength is changed from 457.9 nm (Figure 3d) to 488.0 nm (figure 3e).

With $(bpy)_2Ru(dpp)Ru(bpy)_2^{4+}$, the results are similar but are more explicit since the visible absorption bands are better resolved. As the excitation wavelength approaches the 425-nm absorption maximum, Raman-active vibrations characteristic of coordinated bpy dominate the spectrum while vibrations attributed to dpp increase in relative intensity as the excitation wavelength approaches and passes to the long-wavelength side of the 520-nm absorption. The ratio of intensities of the 1473-cm^{-1} dpp vibration to the 1494-cm^{-1} bpy vibration increases from 0.33 to 1.0 when the excitation wavelength is increased from 457.9 nm (Figure 3b) to 514.5 nm (Figure 3c). The dependence of vibrational intensity on excitation wavelength establishes that the 425- and 525-nm absorptions of the bimetallic complex correspond to the 430-nm absorption maximum and 470-nm shoulder of the monometallic analogue, respectively.

Electrochemical Measurements. Cyclic voltammograms of deaerated acetonitrile solutions with 0.1 M tetraethylammonium perchlorate containing 5×10^{-4} M $[Ru(bpy)_2(dpp)](ClO_4)_2$ (Figure 4a) show single anodic and cathodic peaks. Plots of log $(i/(i_d - i))$, where i and i_d are the currents at an applied voltage, V, and the diffusion-limited current, respectively, vs. V[34,35] are linear with slopes of 0.071 ± 0.004 for the anodic sweep and 0.041 ± 0.007 for the cathodic sweep. Under identical conditions, the cyclic voltammograms of $[Ru(bpy)_3](ClO_4)_2$ yield slopes of 0.063 ± 0.007 for the anodic sweep and 0.044 ± 0.014 for the cathodic sweep. The agreement between these last values and those obtained with $Ru(bpy)_2(dpp)^{2+}$ establishes that $Ru(bpy)_2(dpp)^{2+}$ undergoes one-electron oxidation and reduction steps. The separation between the anodic and cathodic peaks, 88 mV, is larger than the theoretical difference of 59 mV, but the ratio of the peak currents, ≥ 0.96, indicates that the one-electron oxidation of $Ru(bpy)_2(dpp)^{2+}$ is reversible. The $E_{1/2}$ value listed in Table II is the average of the anodic and cathodic peak potentials.

Cyclic voltammograms of $(bpy)_2Ru(dpp)Ru(bpy)_2^{4+}$ (Figure 4b) run under the same conditions as those of the monometallic analogue show two anodic and two cathodic peaks. Plots of log $(i/(i_d - i))$ vs. V[34,35] yield slopes of 0.074 ± 0.003 for the first anodic wave and 0.044 ± 0.015 for the corresponding cathodic wave. The second waves yield slopes of 0.036 ± 0.013 for the anodic sweep and 0.043 ± 0.006 for the cathodic sweep. Some of these slopes differ from those found for $[Ru(bpy)_3](ClO_4)_2$, but the difference is attributed, in part,

(31) Bradley, P. G.; Kress, N.; Hornberger, B. A.; Dallinger, R. F.; Woodruff, W. H. *J. Am. Chem. Soc.* **1981**, *103*, 7441.
(32) Basu, A.; Gafney, H. D.; Strekas, T. C. *Inorg. Chem.* **1982**, *21*, 2231.
(33) Dallinger, R. F.; Woodruff, W. H. *J. Am. Chem. Soc.* **1979**, *101*, 4391.
(34) Headridge, J. B. "Electrochemical Technique for Inorganic Chemists"; Academic Press: London, 1969; Chapter 3.
(35) Piekarske, S.; Adams, R. N. *Tech. Chem. (N.Y.)* *1* (Part IIA).

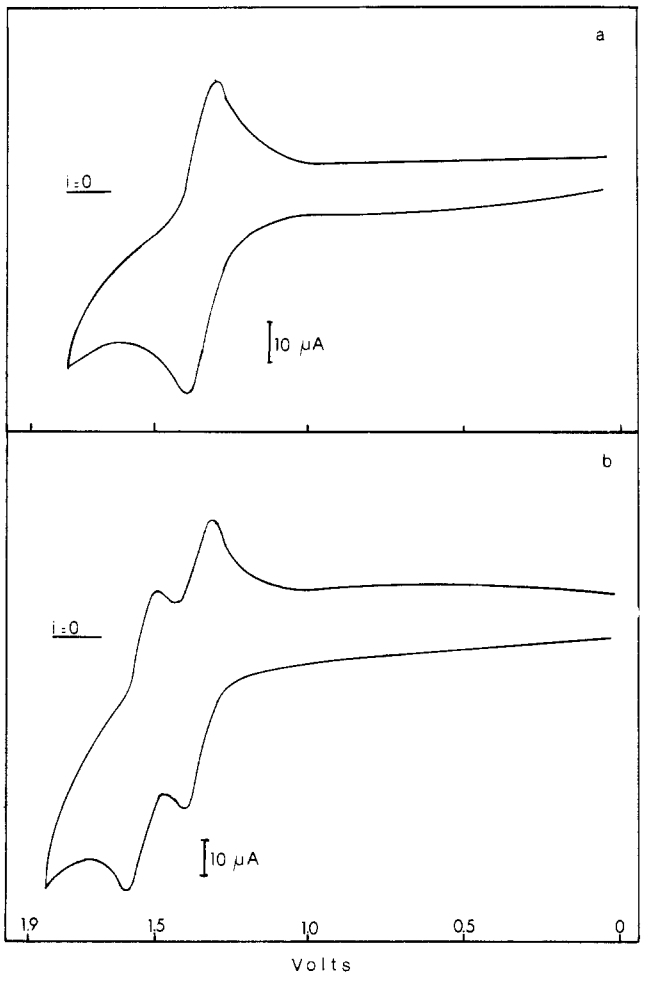

Figure 4. Cyclic voltammograms for (a) $(bpy)_2Ru(dpp)^{2+}$ and (b) $(bpy)_2Ru(dpp)Ru(bpy)_2^{4+}$ in acetonitrile (working electrode Pt microcylinder, reference electrode Ag/AgCl, scan rate 200 mV/s).

to an uncertainty in resolving the individual waves. Since the slopes obtained from the first anodic wave and second cathodic wave are within experimental error of those for $Ru(bpy)_3^{2+}$, however, these data are taken as evidence of individual, sequential, one-electron redox steps. The separation between the anodic peak and its corresponding cathodic peak is 95 mV for the first oxidation and 98 mV for the second oxidation. As found with the monometallic analogue, however, the ratio of the peak currents, ~0.95, suggests that both first and second oxidations of $(bpy)_2Ru(dpp)Ru(bpy)_2^{4+}$ are reversible. The $E_{1/2}$ values listed in Table II for each one-electron oxidation of $(bpy)_2Ru(dpp)Ru(bpy)_2^{4+}$ are the average of the anodic and corresponding cathodic peak potentials. The first (2+,2+ → 2+,3+) and second (2+,3+ → 3+,3+) oxidation potentials of $(bpy)_2Ru(dpp)Ru(bpy)_2^{4+}$ are similar to the potentials of the analogous 2,2′-bipyrimidine[14-16] and 4,4′-dimethyl-2,2′-bipyrimidine[14] bimetallic $Ru(bpy)_2^{2+}$ complexes. Yet, unlike these last bimetallics, where the first oxidation potential of the bimetallic complex differs by 0.15–0.18 V from the oxidation potential of the corresponding monometallic analogue,[14] the potentials listed in Table II show that the first oxidation potential of $(bpy)_2Ru(dpp)Ru(bpy)_2^{4+}$ is within experimental error of the oxidation potential of $Ru(bpy)_2(dpp)^{2+}$.

Cyclic voltammograms of the free ligand dpp, under the same conditions of those of the mono- and bimetallic complexes, show no oxidative wave and indicate that oxidation of dpp occurs at a potential greater than 2.0 V.

The one-electron oxidation waves of the dinuclear complex and their separation indicate that the 2+,3+ mixed-valence complex is accessible by Ce^{4+} oxidation. To carry out the oxidation, a 3-mL aliquot of a 0.2 M D_2SO_4/D_2O solution 10^{-3} M in $(bpy)_2Ru(dpp)Ru(bpy)_2^{4+}$ was placed in a 1-cm optical cell. Aliquots of titrant, 0.2 M ceric ammonium sulfate standardized with As_2O_3 according to the procedure of Vogel,[36] were added with a syringe, and spectra were recorded after each addition. The initial absorbance characteristic of the 2+,2+ bimetallic declines in proportion to the amount of Ce^{4+} added, but there is no concurrent increase in absorbance, $\Delta A \leq 0.01$, in the 600–2000-nm region attributable to the 2+,3+ mixed-valence complex. We estimate that an IT band with $\epsilon \geq 10$ M^{-1} cm^{-1} would be detected in our experiments. Unfortunately, secondary reactions cloud the interpretation of these results. After oxidation, excess $NaNO_2$ was added to reduce the mixed-valence complex and regenerate the original 2+,2+ complex. Although $NaNO_2$ quantitatively reduces $Ru(bpy)_3^{3+}$ to $Ru(bpy)_3^{2+}$, reduction of the Ce^{4+} oxidation product regenerates <10% of the original 2+,2+ bimetallic complex. Spectra recorded after reduction show that the reduction product has a 470-nm absorption band similar to that of $Ru(bpy)_2(dpp)^{2+}$. Since these results suggest that the mixed-valence complex is cleaved, we hesitate to claim, although we have not been able to detect it, that an IT band is not present in the mixed-valence complex. It seems likely that the near-IR absorption of the 5+ ion (IT band) must have $\epsilon \leq 10$ M^{-1} cm^{-1} to escape detection in our experiments. The time scale of the "cleavage" of this ion was not directly measured but occurs within the time needed to add nitrite, shake the solution, and record a spectrum (ca. 3 min).

Discussion

The visible absorption spectra of $Ru(bpy)_2(dpp)^{2+}$ and $(bpy)_2Ru(dpp)Ru(bpy)_2^{4+}$ (Figure 1) resemble the visible absorption spectra of other Ru(II) polypyridine complexes in which the absorptions are assigned to $d-\pi^*$ MLCT transitions. However, the vibrational modes resonant with the optical absorptions of $Ru(bpy)_2(dpp)^{2+}$ and $(bpy)_2Ru(dpp)Ru(bpy)_2^{4+}$ exhibit a pronounced dependence on the excitation wavelength, which indicates that the visible MLCT transitions of these complexes terminate in different ligands.

The resonance Raman spectra of $Ru(bpy)_2(dpp)^{2+}$ in Figure 3 show, in addition to the seven bpy vibrations, three vibrations at 1266, 1473, and 1519 cm^{-1}. These three are assigned to dpp vibrations since they occur within the region expected for diimine deformations but are not present in the spectrum of $Ru(bpy)_3^{2+}$. Since the bpy vibrational intensity approaches a maximum when the excitation wavelength overlaps the 425-nm absorption, this absorption is assigned, assuming O_h microsymmetry, to a $t_2-\pi^*$ MLCT transition where the π^*-acceptor orbital is principally localized on the bpy ligand. Moving the excitation wavelength across the 480-nm shoulder increases the intensity of the dpp vibrations relative to the intensities of the bpy vibrations. The 480-nm transition is therefore assigned to a $t_2-\pi^*$ MLCT transition where the π^*-acceptor orbital is principally localized on the dpp ligand.

The resonance Raman spectra of $(bpy)_2Ru(dpp)Ru(bpy)_2^{4+}$ in Figure 3 show a similar dependence on excitation wavelength. Excitation of the bimetallic complex with 457.9-nm light, which falls within the 425-nm absorption, yields a spectrum dominated by the vibrations of bpy. Increasing the excitation wavelength from 457.9 nm through the 520-nm absorption increases the ratio of the dpp vibrational intensity relative to the intensity of nearby bpy vibrations from ca. 0.3 to 1.0. Consequently, the 425-nm absorption is assigned to a $t_2-\pi^*$ MLCT transition that terminates in a π^* orbital principally localized on the bpy ligand, whereas the 525-nm absorption, also a $t_2-\pi^*$ MLCT transition, terminates in a π^*

(36) Vogel, A. I. "A Text-Book of Quantitative Inorganic Analysis"; Wiley: New York, 1961; pp 315–326.

orbital principally localized on the dpp bridging ligand.

The spectral data indicate that coordination of $Ru(bpy)_2^{2+}$ onto $Ru(bpy)_2(dpp)^{2+}$ to form the bimetallic complex lowers the energy of the MLCT transition to the dpp π^* orbital 1600 cm^{-1}. Similarly, the uncorrected emission maximum shifts from 675 nm for $Ru(bpy)_2(dpp)^{2+}$ to 755 nm for $(bpy)_2Ru(dpp)Ru(bpy)_2^{4+}$. Since the decrease in emission energy, 1600 cm^{-1}, is equivalent to the change in energy of the MLCT absorptions, the emission in both mono- and bimetallic complexes is assigned to π^*–t_2 transitions where the π^* orbital is localized on the dpp ligand. The relative emission quantum yields listed in Table I are independent of the excitation wavelength. Regardless of the state initially populated on absorption, i.e., whether the charge is initially transferred to a π^* orbital on bpy or dpp, both states undergo internal conversion with equal efficiency to an emissive state where the charge is localized on the dpp ligand.

In these Ru(II) complexes, where the spin–orbit coupling of the metal ion blurs the distinction of spin states,[37] internal conversion, which allows energy degradation through the vibrational manifolds of the different excited states, is thought to occur by vibrational mixing and is proportional to the Franck–Condon factor describing the overlap of the vibrational states.[38,39] The Raman intensities of the bpy and dpp vibrations resonant with the optical transitions are a function of excitation wavelength, but no excitation wavelength accessible in these experiments yields a spectrum of only bpy or dpp vibrations. Even for excitation beyond the 525-nm MLCT maximum (i.e., at 570 nm) bpy vibrations at 1607, 1495, and 1323 cm^{-1} show significant residual intensity. A calculation of the resonance Raman intensity dependence for a 1600-cm^{-1} vibration, with a single excited state corresponding to the 425-nm transition, shows expected intensity ratios of 1:0.17:0.08 for 457.9-, 514.5-, and 570.0-nm excitation, respectively.[40] These values have been normalized for fourth-power frequency dependence. Experimental values for the complex $Ru(bpy)_3^{2+}$ agree well with these calculated results. The persistence of bpy vibrations in the spectra excited to the long-wavelength side of the 520-nm peak for the bimetallic complex may indicate some degree of mixing of the excited states via specific vibrations that are responsible for the interconversion of these states discussed with reference to the emission spectra.

The spectral and electrochemical properties of previously synthesized bimetallic Ru(II) complexes indicate significant interaction between the metal ions.[6-16] Dose and Wilson[14] report that the oxidation potential of $Ru(bpy)_2(bpm)^{2+}$ is 1.29 V while the first oxidation potential of $(bpy)_2Ru(bpm)Ru(bpy)_2^{4+}$, i.e., 2+,2+ → 2+,3+, is 1.44 V. The 0.15-V change indicates that coordination of the second $Ru(bpy)_2^{2+}$ moiety to form the bimetallic complex lowers the average energy of the Ru(II) t_2 orbitals by 1210 cm^{-1}. The visible spectrum of $Ru(bpy)_2(bpm)^{2+}$ consists of a broad absorption centered at 420 nm while that of $(bpy)_2Ru(bpm)Ru(bpy)_2^{4+}$ consists of two bands at 408 and 592 nm. Since the ϵ values ($\geq 10^3$ M^{-1} cm^{-1}) are indicative of charge-transfer transitions and the spectra are similar to those of $(bpy)_2Ru(dpp)^{2+}$ and $(bpy)_2Ru(dpp)Ru(bpy)_2^{4+}$, we would assign the 592-nm transition in the spectrum of $(bpy)_2Ru(bpm)Ru(bpy)_2^{4+}$ to an MLCT to the bridging bpm ligand. Coordination of $Ru(bpy)_2^{2+}$ onto $Ru(bpy)_2(bpm)^{2+}$ shifts the MLCT to bpm from ca. 420 to 592 nm. This corresponds to a 6920-cm^{-1} shift,

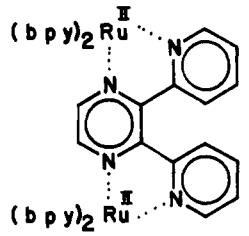

bpy = 2,2'-bipyridine

a

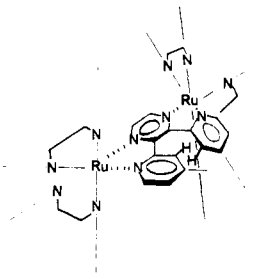

N N = Diimine function of 2,2'-bipyridine

b

Figure 5. (a) Structure of $(bpy)_2Ru(dpp)Ru(bpy)_2^{4+}$. (b) Depiction of the distortion from planarity arising from 3,3'-H,H steric interaction.

which, along with the 1210-cm^{-1} decrease in energy of the Ru(II) t_2 orbitals, implies that coordination of $Ru(bpy)_2^{2+}$ onto $Ru(bpy)_2(bpm)^{2+}$ lowers the energy of the bpm π^*-acceptor orbital by 8130 cm^{-1}. A similar calculation utilizing the spectral and electrochemical properties of $Ru(bpy)_2(4,4'\text{-}Me_2bpm)^{2+}$ (4,4'-Me_2bpm denotes 4,4'-dimethyl-2,2'-bipyrimidine) and $(bpy)_2Ru(4,4'\text{-}Me_2bpm)Ru(bpy)_2^{4+}$ [14] indicates that coordination of the second $Ru(bpy)_2^{2+}$ moiety lowers the energy of the Ru(II) t_2 orbitals by 1450 cm^{-1} and that of the 4,4'-Me_2bpm π^*-acceptor orbital by 6780 cm^{-1}.

While the above bimetallic complexes show significant metal–metal interaction in both ground and excited states, the spectral and electrochemical properties of $Ru(bpy)_2(dpp)^{2+}$ and $(bpy)_2Ru(dpp)Ru(bpy)_2^{4+}$ indicate only slight changes in the orbital energies. The potentials listed in Table II show that the oxidation potential of $Ru(bpy)_2(dpp)^{2+}$ is equivalent to the first oxidation potential of $(bpy)_2Ru(dpp)Ru(bpy)_2^{4+}$ which implies that the Ru(II) t_2 orbital energy is unchanged in the bimetallic complex. Consequently, the shift in the band maximum of the MLCT to the dpp ligand, from 480 nm in $Ru(bpy)_2(dpp)^{2+}$ to 520 nm in $(bpy)_2Ru(dpp)Ru(dpy)_2^{4+}$, is due largely to a 1600-cm^{-1} decrease in the energy of the dpp π^*-acceptor orbital. While other effects should be considered in an exact evaluation of these energy level changes, the qualitative difference between the dpp case and the bpm case is clear. These changes in orbital energies that occur when $Ru(bpy)_2^{2+}$ is coordinated onto $Ru(bpy)_2(dpp)^{2+}$ are similar to those induced by a weak electron-withdrawing substituent rather than a strong metal–metal interaction. Relative to the oxidation potential and MLCT band maximum of $Ru(bpy)_3^{2+}$, for example, substitution of triethylphosphonium, $-P(C_2H_5)_3^+$, onto the 4-position of bpy to form $Ru(4\text{-}Et_3P(bpy))_3^{5+}$ decreases the oxidation potential by 0.23 V and shifts the MLCT band maximum to 466 nm.[41] These data indicate a 1860-cm^{-1}

(37) Crosby, G. A.; Hipps, K. W.; Elfring, W. H., Jr. *J. Am. Chem. Soc.* **1974**, *96*, 629.
(38) Robinson, G. W.; Frosch, R. P. *J. Chem. Phys.* **1962**, *37*, 1962; **1963**, *38*, 1187.
(39) Birks, J. B. "Photophysics of Aromatic Molecules"; Wiley-Interscience: New York, 1970; p 149.
(40) Albrecht, A. C.; Hutley, M. C. *J. Chem. Phys.* **1971**, *55*, 4438.

Table II. Voltammetric Data for the Ruthenium(II) Complexes in Acetonitrile[a]

complex	$E_{1/2}$(an), V		$E_{1/2}$(cat), V		E_p, mV	
	I	II	I	II	I	II
$(bpy)_2Ru(dpp)^{2+}$	+1.540	...	+1.619	...	88	...
$(bpy)_2Ru(dpp)Ru(bpy)_2^{4+}$	+1.548	+1.743	+1.584	+1.770	95	98
$Ru(bpy)_3^{2+}$	+1.380	...	+1.424	...	97	...
free ligand dpp	≥2.0					

[a] Half-wave potentials measured at 23 ± 2 °C at a Pt button electrode in deaerated 5×10^{-4} M solutions of the complexes, with 0.1 M tetraethylammonium perchlorate as the supporting electrolyte. The half-wave potentials ($E_{1/2}$) are reported vs. the standard hydrogen electrode. bpy = 2,2'-bipyridine.

decrease in the energy of the Ru(II) t_2 orbitals and a 2510-cm^{-1} decrease in the energy of the π^*-acceptor orbital. Also, the dpp vibrations that occur at 1266 and 1519 cm^{-1} in the resonance Raman spectrum of $Ru(bpy)_2(dpp)^{2+}$ appear as split bands at 1244, 1259 cm^{-1} and 1562, 1567 cm^{-1}, respectively, in the spectrum of $(bpy)_2Ru(dpp)Ru(bpy)_2^{4+}$. The splitting is reminiscent of the pattern found with asymmetrically substituted bipyridine complexes. These relatively small changes in the orbital energies and the splittings in the resonance Raman spectrum that occur when $Ru(bpy)_2^{2+}$ is coordinated onto $Ru(bpy)_2(dpp)^{2+}$ suggest that in the bimetallic complex the second $Ru(bpy)_2^{2+}$ moiety can be viewed as a weak electron-withdrawing substituent.

Clearly, the difference between this bimetallic dpp complex, which is luminescent in room-temperature fluid solution, and the bimetallic bpm complexes, which are not, is the perturbation caused by the second $Ru(bpy)_2^{2+}$ moiety. The data are not sufficient to specify the exact cause and effect relationship, but the general pattern found with the bimetallic complexes appears to parallel that found with substituted tris(polypyridine)ruthenium(II) complexes. In those complexes where the substituent exerts a large perturbation, particularly on the π^*-acceptor orbital, the luminescent lifetime and emission intensity either are significantly reduced or are nondetectable. Relative to $Ru(phen)_3^{2+}$ (phen denotes 1,10-phenanthroline), for example, substitution of an NO_2 group onto the 5-position decreases the emission lifetime from 920 ± 100 ns for $Ru(phen)_3^{2+}$ to ≤5 ns for $Ru(5\text{-}NO_2phen)_3^{2+}$, as well as decreases the emission intensity.[42] When NO_2 is substituted onto the 4-position of bpy, no emission is detected from room-temperature fluid solutions of $Ru(4\text{-}NO_2bpy)_3^{2+}$.[41] Relative to $Ru(bpy)_3^{2+}$, the NO_2 group lowers the energy of the π^*-acceptor orbital by 3570 cm^{-1}, and resonance Raman spectra indicate that, in the excited state, a significant portion of the charge is localized on the NO_2 group, which is strongly coupled to the solvent medium.[41] The latter then allows an efficient radiationless deactivation of the excited complex. In the bimetallic complexes where significant metal–metal interaction occurs in the excited state, the π^*-acceptor orbital may be distorted toward the second metal center, which, if coupled to the solvent, may offer an efficient pathway for radiationless deactivation.

The relatively small changes in orbital energies, which suggest a relatively small metal–metal interaction in $(bpy)_2Ru(dpp)Ru(bpy)_2^{4+}$, are attributed to steric constraints imposed by the bridging dpp ligand. In the bimetallic bpm complexes, the Ru(II) ions are relatively close and the equatorial coordination planes, i.e., the planes defined by the Ru(II) ion and the coordinating nitrogens of the bpm ligand, are essentially coplanar. Both structural conditions—short distance and planarity—facilitate an interaction between the metal ions.

The distance between the Ru(II) ions in $(bpy)_2Ru(dpp)Ru(bpy)_2^{4+}$ is larger than that in $(bpy)_2Ru(bpm)Ru(bpy)_2^{4+}$. Nevertheless, the smaller interaction found in the former can not be simply due to the larger metal–metal distance since Rillema and Meyer[16] have reported that the bimetallic complex $(bpy)_2Ru(dpq)Ru(bpy)_2^{4+}$ (dpq denotes 2,3-bis(2-pyridyl)-quinoxaline) is not luminescent in room-temperature fluid solution. The ligand dpq differs from dpp only in having a benzo ring fused on to the bridging pyrazine ring, and the distances between the Ru(II) ions in both the bimetallic dpq and dpp complexes are identical. In $Ru(bpy)_2(dpp)^{2+}$, one pyridine ring of dpp can be orthogonal to the plane of the other pyridine and pyrazine rings, but in the formation of the bimetallic complex, both pyridine rings are forced toward planarity with the pyrazine ring. As indicated by the structure of dpp in Figure 5a, this causes significant steric crowding between the hydrogens on the pyridine rings. Molecular models confirm the steric crowding and suggest, as shown in Figure 5b, that planes containing the coordinating nitrogens and each Ru(II) ion could be tilted as much as 35–40° relative to each other. Steric crowding of the pyridine hydrogens also occurs in forming the bimetallic complex with dpq. However, molecular models suggest that the quinoxaline function is less flexible and that twisting of this bridging ligand is less pronounced. Since the extent of interaction between resonant π systems follows cos θ, where θ is the torsional angle between the planes of each system, the interaction will not monotonically decrease as θ increases. Rather, a relatively large θ is needed to significantly reduce the metal–metal interaction to that of a weak electron-withdrawing substituent. In our opinion, the relatively large twisting of the dpp bridging ligand is the reason for the relatively small interaction between the metal ions in this bimetallic complex.

Additional bridging ligands are being synthesized to further test these ideas regarding ligand distortion, metal–metal interaction, and luminescence.

Conclusion

The effect of coordinating $Ru(bpy)_2^{2+}$ onto $Ru(bpy)_2(dpp)^{2+}$ is similar to that of substituting a weak, electron-withdrawing substituent onto the periphery of $Ru(bpy)_3^{2+}$. The occurrence of luminescence from both mono- and bimetallic complexes suggests that luminescence from a bimetallic Ru(II) complex demands relatively little metal–metal interaction.

Acknowledgment. H.D.G. thanks the Andrew W. Mellon Foundation for a fellowship, 1981–1982, and Dr. Ben Tefertiller for a very enjoyable stay at the Dow Chemical Co. laser laboratory. Support of this research by the Research Foundation of the City University of New York, the Dow Chemical Co. Technology Acquisition Program, and the donors of the Petroleum Research Fund, administered by the American Chemical Society, is also gratefully acknowledged. A.D.B. acknowledges support through a PSC-BHE grant (No. 13921) from the Research Foundation of the City University of New York.

Registry No. $[(bpy)_2Ru(dpp)](ClO_4)_2$, 88635-48-7; $[(bpy)_2Ru(dpp)Ru(bpy)_2](ClO_4)_4$, 88635-49-8; *cis*-$Ru(bpy)_2Cl_2$, 19542-80-4; dpp, 25005-96-3; ethylenediamine, 107-15-3; 2,2'-pyridil, 492-73-9; 2,3-bis(2-pyridyl)-5,6-dihydropyrazine, 25005-95-2.

(41) Basu, A.; Weiner, M.; Strekas, T. C.; Gafney, H. D. *Inorg. Chem.* **1982**, *21*, 1085.
(42) Lin, C. T.; Bottcher, W.; Chou, M.; Creutz, C.; Sutin, N. *J. Am. Chem. Soc.* **1976**, *98*, 6536.